PROCEEDINGS OF SCIENCE

Galactic cosmic-rays and habitable planets

R. Brose[a,*] **and M. D. Filipović**[b]

[a] *Dublin Institute for Advanced Studies, Astronomy & Astrophysics Section, DIAS Dunsink Observatory, Dublin D15 XR2R, Ireland*

[b] *Western Sydney University, Locked Bag 1797, Penrith, NSW, 2751, Australia*

E-mail: broserob@cp.dias.ie

The question if there is life on other planets has fueled a decade full of exciting discoveries in the field of exo-planet research. The number of known exoplanets has grown beyond 5,000 till today and with the launch of the James Webb Space Telescope, we are now able to probe the atmospheres of the most nearby systems directly, allowing to search for tracers of life.

However, most of the current approaches of finding life are based on a “follow-the-water” strategy. Here, we present a different approach by studying the impact of Galactic cosmic-rays (CRs) on potentially habitable planets around Sun-like stars. Most of the CRs that interact with the Earth's atmosphere originate directly from the Sun. Due to their low-energy they get absorbed high in the atmosphere and contribute little to the radiation-dose we receive at the surface. On the other hand, the Galactic CR spectrum extends to much higher energies allowing the particle-induced cascades to reach ground level and directly impact life.

The detection of very-high energy gamma-ray emission from stellar clusters has increased number of source classes known to accelerate cosmic-rays at least up into the TeV domain to four. We use observational data of the gamma-ray emission from Supernova remnants, colliding-wind binaries, young and massive stellar clusters and the Galactic center to infer the CR density around these sources and determine distances up too which life gets affected by the produced CRs for a “twin” of our solar system.

38th International Cosmic Ray Conference (ICRC2023)
26 July - 3 August, 2023
Nagoya, Japan

[*] Speaker

PoS(ICRC2023)441

1. Introduction

Earth is the only planet in our universe known to host life. However, even on Earth the conditions for supporting life are not stable since fossil records show that (mass)-extinction events are quite common in Earth's history. While the most famous of those events - the Cretaceous–Paleogene extinction event 66 million years ago - is likely linked to the impact of an asteroid, the origin of the other extinction events remains unclear. A number of studies have been conducted to link these extinction events with astrophysical events and processes. There seems to be a correlation between the occurrence extinction events with the passage of our solar system in and out of the spiral arms of our Galaxy [10].

The spiral arms of our Galaxy are rich in young and massive stars and can hence be linked to astrophysical processes that correlate with a high star formation rate. One of these processes is the acceleration of Galactic cosmic rays (CRs), that were long believed to be produced by supernova remnant (SNR) shocks. However, lately more objects, like young stellar clusters [2], the Galactic center region [15] or colliding wind binaries [14] were identified to efficiently accelerate particles based on their gamma-ray emission. The occurrence rate of all these objects is linked to the star-formation rate as well.

So far, the connection between CRs and life was mostly based on the low-energy CRs produced by the stars that potential life-hosting planets orbit [23, and references therein]. A high production rate of CRs and/or a high variability of CR production, including strong stellar flares, might impact the atmospheric chemistry and the capability of star-systems to host life. However, the vast majority of the CRs produced by stars themselves gets absorbed in the upper atmosphere. The Galactic sources of CRs on the other hand produce far more energetic particles whose extensive air showers can reach ground-level.

At the present time, the Galactic CRs represent only ≈ 11 % of the radiation dose exposure at sea-level on Earth. However, the CR density around the Galactic sources is orders of magnitude higher and exhibits harder spectra, such that a far higher radiation dose can be expected close to those sources with potential harmful effects for life-hosting planets. Further, it has been established earlier by [19], that an enhanced CR flux arriving at Earth, e.g. from a close-enough SNR, could change the ionization and chemistry of Earth's lower atmosphere, affecting the climate. Such an event might have played a key role in changing Earth's ecosystems ≈ 2.6 million years ago [19].

2. Local Cosmic ray densities from gamma-ray observations

The gamma-ray emission from Galactic sources can be a valuable tool in determining the CR content in these sources. For many sources, it is not clearly known if the origin of the gamma-ray emission is of leptonic origin via the inverse-Compton process or of hadronic emission by the production of neutral Pions in pp-interactions of accelerated nucleons with dense clouds of gas [e.g. 22, and references therein]. In this work, we assume that the sources are hadronic emitters on grounds of the observational correlation of the gamma-ray emission and tracers of dense gas as CO line emission. As a consequence, the gamma-ray emission can be used to determine the local density of CRs in the region of the sources.

PoS(ICRC2023)441

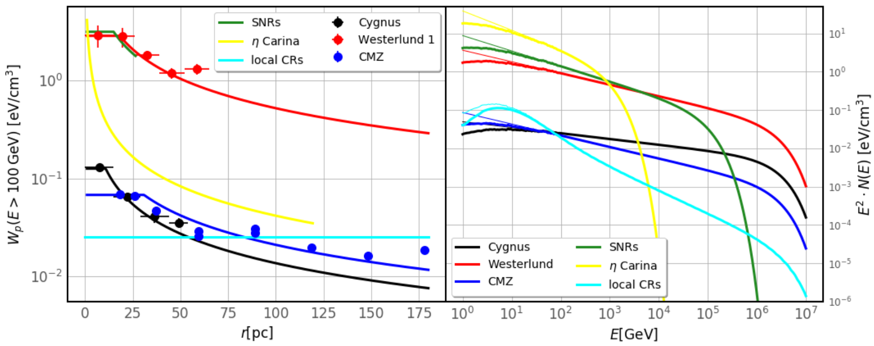

Figure 1: The left panel shows the energy density in CRs above 100GeV for the different CR sources. Points indicate measured CR densities and the lines the prescriptions we adopt. The right panel shows the CR spectra including the effects of stellar modulation (thick lines) and without modulation (thin lines). The local CR data is taken from [25].

We summarized the observational data in Figure 1 and are describing the details of the observations and our assumptions for the models displayed in Figure 1 in the following sections.

2.1 Galactic center

The H.E.S.S. collaboration reported extended gamma-ray emission around the central molecular zone (CMZ) of our Galaxy [15]. Together with surveys of the gas-density based on line-emission of CS, CO and HCN, this allows estimating the local CR density around Sagittarius A*. The spectrum of the gamma-ray emission from all the extraction-regions yields a gamma-ray spectral index of $s \approx 2.3$ with no significant sign of a cut-off at the highest energies.

The analysis of the gamma-ray emission indicates that the CR density is falling as $1/r$ in the vicinity of the CMZ, indicating a scenario of continuous injection of CRs in this region in the past. The CR density is hereby exceeding the local CR density by at least a factor of four up to distances of 180 pc around Sgr A* [15].

As the gamma-ray data is not constraining in this regard, we assume in the following that the CR spectrum has a cutoff a $E_{\rm cut} = 3\,\mathrm{PeV}$. This leaves no detectable imprint of the emission from the CMZ but limit the energy-density in the CRs. Further, that cut-off is in line with observations of the knee of local CR spectrum [25].

2.2 Young massive stellar clusters

[2] used gamma-ray observations of the two young massive stellar clusters Westerlund 1 and Cyg OB2 to derive the CR distribution around both objects. The observations were conducted with Fermi-LAT for Cyg OB2 and additionally H.E.S.S. for Westerlund 1.

Again, both sources show a $1/r$-dependence for the CR density in their vicinity. At the same time, the CR spectra exhibit significantly higher CR densities at energies above $\approx 100\,\mathrm{GeV}$ as compared to the solar neighborhood. The gamma-ray spectra of Westerlund 1 show no sign of a significant cutoff above 100 TeV, so we assume the same $E_{\rm cut} = 3\,\mathrm{PeV}$ as for the Galactic center region.

The emission from Cyg OB2 is detected in high-energy gamma-rays only. As a consequence, also here the cutoff is not constrained and we choose the generic $E_{\rm cut} = 3\,\mathrm{PeV}$. There is a slight difference in the reported spectral index, as Cygnus shows a gamma-ray spectrum with $s \approx 2.15$ while Westerlund shows a slightly softer spectrum with $s \approx 2.3$.

2.3 Supernova remnants

Deriving the CR density around SNRs has proven to be less successful than in the case of stellar clusters or the CMZ. There are several cases where SNRs are directly interacting with close-by molecular clouds [e.g. 16, 24, 28, 30], however, interactions with multiple clouds at different distances or significant extended emission would be needed to constrain the CR distribution in a similar way as for the sources discussed previously.

To nevertheless constrain the the CR distribution, information on the total energy in CRs produced by SNRs, their cutoff energy, spectral index and the diffusion coefficient around SNRs is needed. The works by [9] and [7, 8] have shown that the fast decline of the maximum energy that SNRs can achieve after entering the Sedov-phase is responsible for the formation of steep/soft gamma-ray spectra in evolved SNRs. Still, the spectrum of all produced CRs is close to a spectral index of $s = 2.4$ [7].

Simple energetic arguments require that SNRs inject about 10 % of their kinetic energy - typically $E_{\mathrm{Exp}} = 10^{51}$ erg - in CRs in order to maintain the energy-content of CRs in our Galaxy [e.g. 13]. Deriving the amount of energy that SNRs channel into CRs is not straight forward and ranges from 2 % in escaped CRs for W28 [16], over 3.8 % for γ-Cygni [18] and 6 − 10 % for G045.7-00.4 [30] to values as high as 30 % for W44 [28]. For this work, we assume that the canonical 10^{50} erg gets channeled into CRs for a single SNR over its entire lifetime.

In order to constrain the volume that CRs accelerated in SNRs occupy, we need an estimate for the diffusion coefficient around SNRs. The magnetic field in the vicinity of the SNR shock needs to be amplified beyond the field in the ISM in order to accelerate CRs to high energies [6]. However, observations [11] and numerical simulations [12] indicate that the diffusion of CRs is suppressed in a large volume around the SNR with diffusion coefficient that is ≈ 1 % of that in the ISM. Further, the diffusion properties show a strong temporal and spatial evolution [8]. Here, we assume a diffusion-coefficient that is constant in time and suppressed by a factor of 100 with respect to the diffusion coefficient in the ISM [27].

We assume that the CR density inside the SNR is constant and assume a generic SNR-extension of $R_{\mathrm{SNR}} = 15$ pc. This corresponds to remnants with ages of a few kyrs when they have lost already the majority of the highest energetic particles. We assume that particles escape diffusively to the upstream, which results in a $1/r$ distribution of particles in the upstream

$$N(E,r) = \begin{cases} N_0 E^{-s} & \text{for } r \leq R_{\mathrm{SNR}} \\ N_0 E^{-s} \frac{R_{\mathrm{SNR}}}{r} & \text{for } r > R_{\mathrm{SNR}} \end{cases} . \tag{1}$$

We require that the volume integral over the CR distribution yields 10^{50} erg in CRs within a radius of

$$R_{\mathrm{max}} = \sqrt{D(E_{\mathrm{max}}) \cdot t} \approx 24\,\mathrm{pc} \tag{2}$$

around the SNR for particles of $E_{\mathrm{cut}} = 100$ TeV and $t = 10$ kyrs. An integration of equation (1) yield the total energy in CRs,

$$10^{50}\,\mathrm{erg} \stackrel{!}{=} \frac{N_0 \pi}{s-2} \left[\frac{4}{3} R_{\mathrm{SNR}}^3 + 2 R_{\mathrm{SNR}} \left(R_{\mathrm{max}}^2 - R_{\mathrm{SNR}}^2 \right) \right] \cdot \left[E_0^{2-s} - E_{\mathrm{cut}}^{2-s} \right] , \tag{3}$$

where we adopt $E_0 = 100\,\mathrm{MeV}$ for the minimum energy CRs[1]. This leads to a CR normalization of $N_0 = 8.8 \cdot 10^{-9}\,\mathrm{GeV}^{1.4}\,\mathrm{cm}^{-3}$.

The CR spectrum and CR distribution are plotted in Figure 1. The similarity of the CR distribution between Westerlund 1 and our generic SNR is a coincidence. The larger extension of the emission from Westerlund 1 makes it evident that the total energy in CRs is significantly larger in the case of the stellar cluster. However, middle-aged SNRs are significantly enhancing the local CR density in their immediate vicinity. In the course of the SNR evolution, the CR density will drop as few high-energy particles are added after entering the Sedov-Taylor stage. Also, with time, the diffusion coefficient self-confining the CRs in a halo around the SNR will increase towards the Galactic value and help to distribute the CRs in a larger volume, significantly reducing their density.

2.4 Colliding-wind binaries

Close binary systems of massive stars are known to be bright emitters in the radio, X-ray, HE gamma-rays [17] and as recently detected also in the VHE gamma-ray domain [14].

Models suggest that a considerable fraction of the mechanical wind-luminosity is being transferred to cosmic-rays. An exact constraint on the CR density from observations alone is difficult, as the density in the wind-collision region strongly varies throughout the orbit and as the exact emission region can not be constrained due to the point-like nature of these sources. Hence, we follow a similar approach as for SNRs (see section 2.3).

We assumed that $\approx 10\%$ of the kinetic wind-luminosity gets converted to CRs, as suggested by [29] and we adopted the values for the stellar properties given in that work. We adopt a lifetime of $200,000\,\mathrm{yrs}$ for the system[2] in order to constrain the total energy of CRs in and around the system and the maximum diffusion radius according to equation (2).

The CR spectrum around η-Car is thus given by

$$N(E,r) = \frac{E_{\mathrm{CR}}(2-s)}{2\pi R_{\mathrm{max}}^2 [E_{\mathrm{min}}^{2-s} - E_{\mathrm{max}}^{2-s}]} \frac{E^{-s}}{r} \exp\left(\frac{-E}{E_{\mathrm{max}}}\right), \tag{4}$$

where $E_{\mathrm{max}} = 55\,\mathrm{pc}$, $s = 2.5$, $E_{\mathrm{max}} = 1\,\mathrm{TeV}$ and $E_{\mathrm{min}} = 10\,\mathrm{GeV}$. $E_{\mathrm{CR}} \approx 10^{50}\,\mathrm{erg}$ is calculated as the kinetic wind luminosity times the conversion efficiency of CRs and the age of the system.

3. Cosmic-ray interactions

The CRs in the vicinity of the sources that we consider here interact with the astro-sphere of our hypothetical star-system as well as with the atmosphere of the exoplanet itself. Our approach to both types of interactions is outlined in the following sections.

3.1 Modeling stellar Modulation

The modulation of CRs in our heliosphere is a complex field of studies in itself [see e.g. 21, for a review]. In this work, we adopt the CR modulation at Earth as calculated by [23] and ignore

[1] The CR spectrum at low energies needs to deviate from the one at high energies. However, a direct measurement at these energies is difficult due to solar modulation of CRs

[2] The lifetime is poorly constrained but the anticipated mass-loss suggests an age of more than $30,000\,\mathrm{yrs}$ and the possible WR-companion an age of less than $500,000\,\mathrm{yrs}$.

variations of the modulation due to the solar cycle.We calculated the radiation doses at ground level for the modulated and unmodulated spectra of the sources in section 2 and found that the impact of the modulation is negligible as the primary source of radiation at ground level is CRs with energies above ≈ 50 GeV (see section 3.2.

3.2 Radiation dose estimation

CRs hitting the Earth's atmosphere will interact usually at a few 10s of km above the ground and produce extended air showers (EAS) [3]. The interaction height depends on the energy and the type of the primary CR. In general, showers originating from a higher energetic primary will propagate deeper into the atmosphere and more secondaries besides muons will reach ground level. These air showers are a well-known source of radiation and contribute, depending on the altitude, about 300 – 1000 μSv [e.g. 32] per year. Depending on the region of the world, this contributes 10 – 20 % to the total absorbed radiation dose.

To evaluate the effect that the CRs around Galactic CR sources will have on the annual radiation dose, we used the AtRIS code [4] to simulate the interaction of CR protons with the Earth's atmosphere. AtRIS is based on the Geant4 [1] code to model nuclear interactions. We used the standard atmosphere model of [20] and modeled the interaction of 120,000 primary protons with energies between 1 MeV and 1 TeV. AtRIS assumes a flat source-spectrum that then has to be folded with the primary CR spectrum to obtain the absorbed dose. We used the standard ICRU water phantom to calculate the absorbed dose [33].

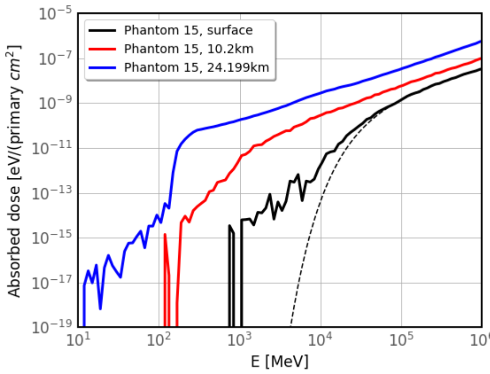

Figure 2: The figure shows the response function (absorbed dose per primary of energy E) for the standard ICRU water phantom at three different heights above the Earth's surface. The thin dashed line represents an analytic fit (see text for details).

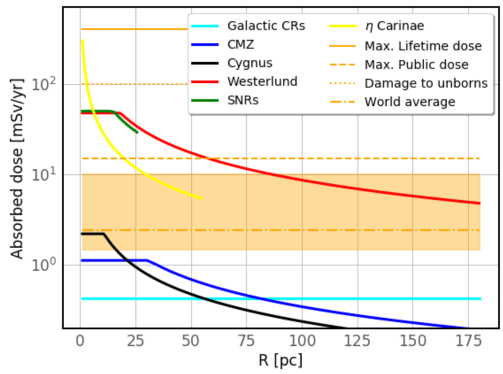

Figure 3: The panel shows the absorbed annual dose at ground level depending on the distance of several CR sources. The horizontal lines indicate the current dose from Galactic CRs (cyan) and the dose limits considered from radiation-protection considerations.

Figure 2 illustrates the response-function, e.g. the energy absorbed in the ICRU-sphere per primary CR of a given energy per cm^2 cross section area of the absorber. Due to computational restrictions, we cannot simulate the interactions over the full energy-range of the primary expected CRs from the Galactic CR sources. However, at higher energies the response function follows a power-law with an exponential suppression towards lower energies. We fitted the response at sea level with

$$f_R(E) = A \cdot \left(\frac{E}{E_0}\right)^s \cdot \exp\left(-\frac{E_0}{E}\right). \tag{5}$$

We estimated the absorbed dose for the Galactic CR spectrum for the full numerical response function and our fit. The doses of $H_{\mathrm{numeric}} = 440\,\mathrm{mSv}$ and $H_{\mathrm{fit}} = 400\,\mathrm{mSv}$ agree reasonably well, so that the fit was used for the dose-estimate throughout the paper.

4. Results and discussion

We calculated the absorbed dose at surface level for the different CR sources depending on the distance to the source and compared the annual radiation dose to various reference doses in figure 3. The absorbed dose for all objects exceeds the current dose caused by Galactic CRs. Further, the absorbed dose for SNRs, η-Car and Westerlund 1 exceeds the the dose from all natural radiation sources on Earth combined for distances below 25 pc.

At distances closer than 20 pc the dose for these three objects exceeds the maximum dose recommended for the general public within a year and within $\approx$ 10 years the recommended lifetime dose due to radiation exposure at the workplace. It has to be noted that all of the above doses-limits are derived for one-time radiation exposures [31].

4.1 Health effects on humans

The effects of increased background-radiation are best-studied for humans. However, establishing conclusive results on the effects of increased background radiation on mortality and cancer rates has proven difficult [26, and references therein]. Studies on the effects of patients exposed to the X-ray contrast medium Thorotrast, where the long half-life of the thorium-232 leads to an increased, lifelong α-particle exposure, showed that the median life-expectancy was lowered by 14 years [5]. The same trend persisted in atomic bomb survivors and workers of the Oak Ridge National Laboratory but the change in rates of cancer mortality shows evidence of sensitivity to the age of the low-level radiation exposure [26, and references therein]. In general, the effects of radiation exposure are weaker for ages between 20-45 years, whereas exposure at younger or older age shows stronger effects. However, studies for the effects of low-level radiation exposure at young ages obviously lack data.

Still, the doses received in the studies mentioned here are lower by a factor of 5-10 compared to the radiation levels that we expect close to SNRs, binaries and stellar clusters. The typical doses received by atomic bomb survivors will be reached within $\approx$ 10 years around those CR sources.

4.2 Ecologic effects

The doses that we predict for our five CR source-classes are too low to cause sterilization of planets or mass extinction by the direct effect of the CRs, even though significantly enhanced cancer-induced mortality and increased levels of mutation and fetal damage might be expected. However, it has been discussed that CRs can yield secondary effects on Earth-like planets by altering the ionization rate of the lower atmosphere. [19] showed that a SNR (or a series of SNRs) located at 50 pc from Earth might have altered the atmosphere's conductivity and hence the rate of lightning and consequently wildfires. Their line of reasoning is supported by ^{60}Fe deposits in sediments that coincide with soot and other carbon-related sediments. These sediments are associated with a period of conversion of woodland to savanna across various continents, which in fact might have supported the development of bipedalism in hominids.

PoS(ICRC2023)441

The CR doses and hence ionization rates, that we calculated in this work are in line with values of [19] and show that also nearby binary systems or massive star clusters might affect the climate of Earth-like planets in a similar way, severely impacting ecosystems and eventually leading to (mass)-extinction events.

5. Conclusions

We obtained the CR density around the CMZ, the star clusters Westerlund 1 and Cyg OB2, SNRs and the colliding-wind binary η-Car and used those distributions to calculate the absorbed radiation dose at sea level for an Earth-like exoplanet.

We find that the obtained doses are enhanced by at least a factor of ten compared to the radiation dose imposed by the Galactic CRs at Earth's surface. At distances of less than 25 pc to SNRs, colliding-wind binaries or star clusters like Westerlund 1, the radiation dose exceeds the Galactic-CR dose by a factor of at least 100 and would become the primary source of radiation on an Earth-like planet.

While this radiation level certainly affects Earth-like life by an enhancement of cancer rates and cancer-induced mortality, the direct effects are not strong enough to cause extinction events. However, indirect effects on the climate such as increased lightning rates due to the enhanced ionization of the atmosphere at sea-level, have the potential to cause strong shifts in the ecosystems and hence potential (mass)-extinction events if exoplanets have close encounters with SNRs, colliding-wind binaries or star clusters like Westerlund 1. In this work we have not yet calculated the frequency with which an Earth-like planet should expect to encounter one of these classes of sources. This is a non-trivial task depending on location in the Galaxy, and will be investigated in future work.

Acknowledgments

R. Brose acknowledges funding from the Irish Research Council under the Government of Ireland Postdoctoral Fellowship program.

References

[1] Agostinelli S., et al., 2003, Nuclear Instruments and Methods in Physics Research A, 506, 250

[2] Aharonian F., Yang R., de Oña Wilhelmi E., 2019, Nature Astronomy, 3, 561

[3] Auger P., Ehrenfest P., Maze R., Daudin J., Fréon R. A., 1939, Reviews of Modern Physics, 11, 288

[4] Banjac S., Herbst K., Heber B., 2019, Journal of Geophysical Research (Space Physics), 124, 50

[5] Becker N., Liebermann D., Wesch H., Van Kaick G., 2008, European Journal of Cancer, 44, 1259–1268

[6] Blandford R., Eichler D., 1987, Physics Reports, 154, 1

[7] Brose R., Pohl M., Sushch I., Petruk O., Kuzyo T., 2020, A&A, 634, A59

[8] Brose R., Pohl M., Sushch I., 2021, A&A, 654, A139

[9] Celli S., Morlino G., Gabici S., Aharonian F. A., 2019, MNRAS, 490, 4317

[10] Filipovic M. D., Horner J., Crawford E. J., Tothill N. F. H., White G. L., 2013, Serbian Astronomical Journal, 187, 43

[11] Fujita Y., Ohira Y., Tanaka S. J., Takahara F., 2009, ApJ, 707, L179

[12] Fujita Y., Ohira Y., Takahara F., 2010, ApJ, 712, L153

[13] Gaisser T. K., 1990, Cosmic rays and particle physics. Cambridge University Press

[14] H. E. S. S. Collaboration et al., 2020, A&A, 635, A167

[15] HESS Collaboration et al., 2016, Nature, 531, 476

[16] Hanabata Y., et al., 2014, ApJ, 786, 145

[17] Humphreys R. M., Martin J. C., 2012, in Davidson K., Humphreys R. M., eds, Astrophysics and Space Science Library Vol. 384, Eta Carinae and the Supernova Impostors. p. 1, doi:10.1007/978-1-4614-2275-4_1

[18] MAGIC Collaboration et al., 2020, arXiv e-prints, p. arXiv:2010.15854

[19] Melott A. L., Thomas B. C., 2019, Journal of Geology, 127, 475

[20] Picone J. M., Hedin A. E., Drob D. P., Aikin A. C., 2002, Journal of Geophysical Research (Space Physics), 107, 1468

[21] Potgieter M. S., 2013, Living Reviews in Solar Physics, 10, 3

[22] Reynolds S. P., 2008, ARA&A, 46, 89

[23] Rodgers-Lee D., Vidotto A. A., Taylor A. M., Rimmer P. B., Downes T. P., 2020, MNRAS, 499, 2124

[24] Tang X., 2019, MNRAS, 482, 3843

[25] Thoudam S., Rachen J. P., van Vliet A., Achterberg A., Buitink S., Falcke H., Hörandel J. R., 2016, A&A, 595, A33

[26] Tong J., Hei T. K., 2020, Radiation Medicine and Protection, 1, 15–23

[27] Trotta R., Jóhannesson G., Moskalenko I. V., Porter T. A., Ruiz de Austri R., Strong A. W., 2011, ApJ, 729, 106

[28] Uchiyama Y., Funk S., Katagiri H., Katsuta J., Lemoine-Goumard M., Tajima H., Tanaka T., Torres D. F., 2012, ApJ, 749, L35

[29] White R., Breuhaus M., Konno R., Ohm S., Reville B., Hinton J. A., 2020, A&A, 635, A144

[30] Zhang H.-M., Liu R.-Y., Su Y., Zhu H., Xi S.-Q., Wang X.-Y., 2021, ApJ, 923, 106

[31] for Radiation Protection F. O., , `https://www.bfs.de/EN/topics/ion/radiation-protection/limit-values/limit-values_node.html`

[32] on Radiation Protection N. C., Measurements 2006, NCRP Report No. 160, 160

[33] on Radiation Units I. C., Measurements 1989, Journal of the International Commission on Radiation Units and Measurements, os23